



# Transduction of modified factor VIII gene improves lentiviral gene therapy efficacy for hemophilia A

Received for publication, September 6, 2021, and in revised form, November 3, 2021. Published, Papers in Press, November 10, 2021, <https://doi.org/10.1016/j.jbc.2021.101397>

Jie Gong<sup>1</sup>, Tsai-Hua Chung<sup>1,2</sup>, Jie Zheng<sup>3</sup>, Huyong Zheng<sup>3</sup>, and Lung-Ji Chang<sup>1,2,3,\*</sup> 

From the <sup>1</sup>School of Medicine, University of Electronic Science and Technology of China, Sichuan, China; <sup>2</sup>Shenzhen Geno-Immune Medical Institute, Shenzhen, China; <sup>3</sup>Hematology Center, Beijing Children's Hospital, Capital Medical University, Beijing, China

Edited by Gerald Hart

Hemophilia A (HA) is a bleeding disorder caused by deficiency of the coagulation factor VIII (F8). F8 replacement is standard of care, whereas gene therapy (F8 gene) for HA is an attractive investigational approach. However, the large size of the F8 gene and the immunogenicity of the product present challenges in development of the F8 gene therapy. To resolve these problems, we synthesized a shortened F8 gene (F8-BDD) and cloned it into a lentiviral vector (LV). The F8-BDD produced mainly short cleaved inactive products in LV-transduced cells. To improve F8 functionality, we designed two novel F8-BDD genes, one with an insertion of eight specific N-glycosylation sites (F8-N8) and another which restored all N-glycosylation sites (F8-299) in the B domain. Although the overall protein expression was reduced, high coagulation activity (>100-fold) was detected in the supernatants of LV-F8-N8- and LV-F8-299-transduced cells. Protein analysis of F8 and the procoagulation cofactor, von Willebrand Factor, showed enhanced interaction after restoration of B domain glycosylation using F8-299. HA mouse hematopoietic stem cell transplantation studies illustrated that the bleeding phenotype was corrected after LV-F8-N8 or -299 gene transfer into the hematopoietic stem cells. Importantly, the F8-299 modification markedly reduced immunogenicity of the F8 protein in these HA mice. In conclusion, the modified F8-299 gene could be efficiently packaged into LV and, although with reduced expression, produced highly stable and functional F8 protein that corrected the bleeding phenotype without inhibitory immunogenicity. We anticipate that these results will be beneficial in the development of gene therapies against HA.

Hemophilia A (HA) is an X-linked monogenic coagulation disorder resulting from the genetic deficiency of the factor VIII (F8) gene in the intrinsic coagulation cascade (1). The current treatment of HA is based on protein replacement therapy (PRT) through plasma-derived coagulation factors or recombinant proteins. The limitations of PRT include short half-life, high cost, and life-time requirement of the treatment. Thus, gene therapy has become highly promising for HA (2–5).

The analysis of the human F8 gene revealed an obvious domain structure for the protein, represented as A1-A2-B-A3-C1-C2 (6).

The B domain is encoded by unusually large exons with highly conserved content of asparagine (N)-linked oligosaccharides (7). Miao *et al.* (8) illustrated that a partial B-domain deletion of F8 (F8-BDD), leaving an N-terminal 226-aa-stretch containing six putative asparagine-linked glycosylation sites intact, was able to increase *in vitro* secretion of F8 by 10-fold. Thus, lowering F8-BDD retention in the endoplasmic reticulum (ER) whereas increasing transport to the Golgi is a rational approach to achieving increased secretion (8, 9).

Lentivirus is a class of retroviruses that can infect both dividing and nondividing cells (10, 11). Shi *et al.* (12) reported that the transduction of hematopoietic stem cells (HSCs) using lentiviral vector (LV) expressing F8 could produce a therapeutic level of F8 in HA mice without antibody formation, illustrating that LV can be a valuable tool in F8 gene therapy applications. Here, we applied an advanced LV carrying a universal promoter-driving F8 transgene expression. To improve F8 secretion and function, we modified the glycosylation sites in the B domain based on a codon-optimized F8-BDD construct. The detailed analyses of F8 protein processing, cofactor interactions, secretion and function of these newly engineered F8-BDD constructs, and *ex vivo* blood clotting activities and *in vivo* immunogenicity in F8 knockout mice were presented.

## Results

### Expression and coagulation analysis of full-length F8 versus F8-BDD

To increase expression, the nucleotide sequences of the full-length F8 (flF8) and F8-BDD constructs were selectively codon-optimized and chemically synthesized. All the constructs were cloned into a pEGWI-LV backbone under control of the ubiquitous EF1 $\alpha$  promoter. We used quantitative PCR (qPCR) method to determine vector titer based on vector genomes in transduced 293 cells. The result illustrated that LV-F8-BDD was packaged into LVs at higher efficiencies than LV-flF8 (Fig. 1A), obviously because of the size reduction (7056 versus 4374 nucleotides).

To investigate F8 expression, we transduced myeloid progenitor K562 cells and the collected cell lysates (L) and S under serum-free condition to avoid serum interference as illustrated in Figure 1B. Genomic DNA (gDNA) was extracted from the

\* For correspondence: Lung-Ji Chang, [c@szgimi.org](mailto:c@szgimi.org).

## Improved lentiviral FVIII gene therapy

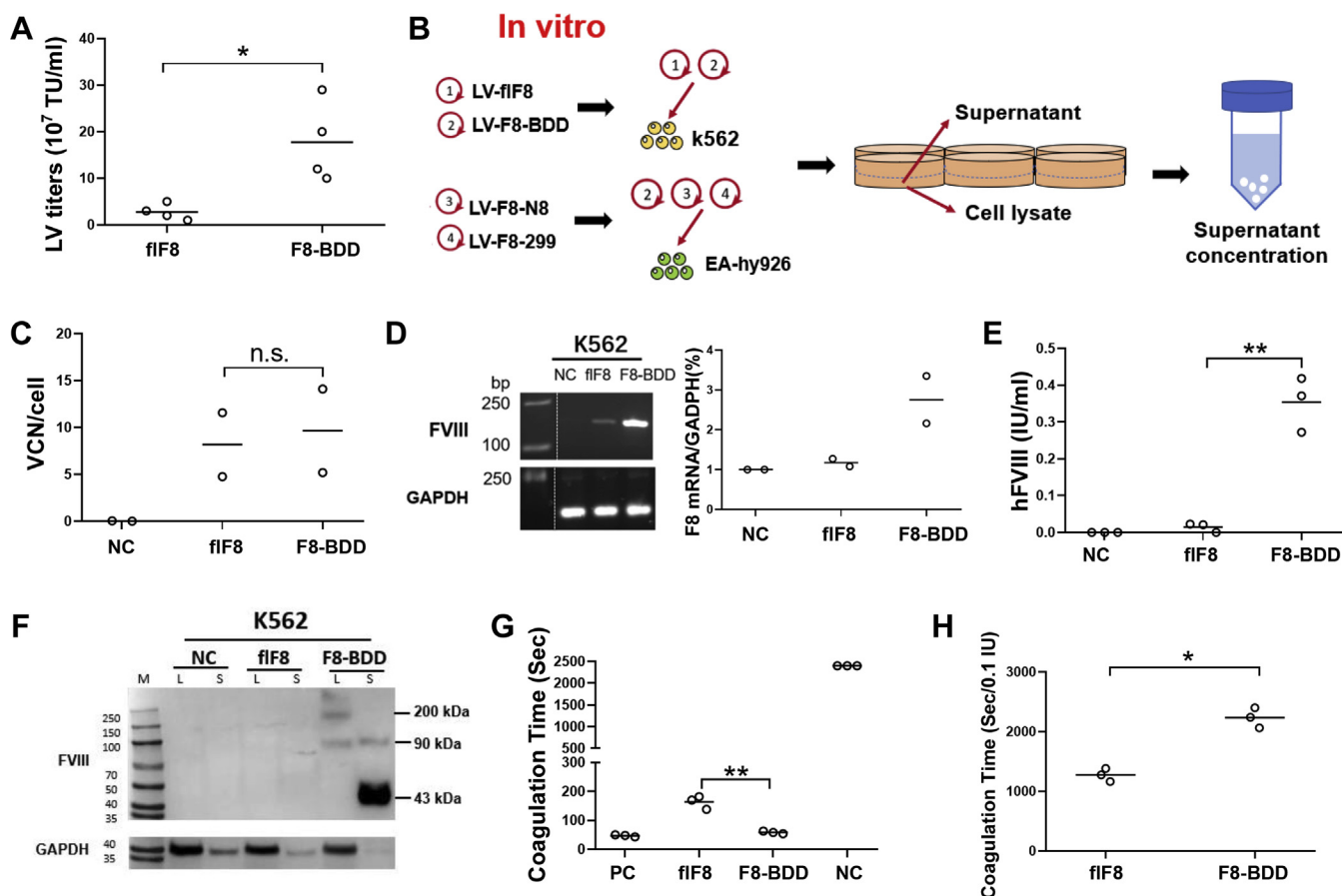


**Figure 1. Analysis of LV-flF8 and -F8-BDD expression and function in K562 cells.** *A*, LV titer comparison. The concentrated LV titers were quantified based on integrated proviral DNA detected by qPCR using gDNA of the transduced cells. *B*, the schematic illustration of *in vitro* transduction of K562 with flF8 and F8-BDD genes. *C*, comparison of VCNs in transduced K562 cells. The VCNs per cell were calculated and plotted. *D*, quantification of F8 RNA expression in K562. RNA RT-qPCR was quantified and shown by representative gel images, and the signal was normalized against internal GAPDH RNA (molecular weight markers ran on the same gel were shown on the *left* and dot plot illustrated on the *right*). *E*, determination of F8 protein concentration of K562-flF8 and K562-F8-BDD using a human coagulation F8 ELISA kit. *F*, WB analysis of F8 proteins in the lysates (L) and supernatants (S) of K562-flF8 and K562-F8-BDD cells, including cleaved products of A2 domain (43-kDa), HC (90-kDa), and LC (80-kDa) as well as a nonprocessed 170-kDa protein. *G* and *H*, *in vitro* F8 functional aPTT assay using F8 deficient plasma. The F8 deficient plasma was mixed with the same volume of supernatants (*G*) or based on the same F8 protein content (*H*) from the K562-flF8 and K562-F8-BDD cells, and the coagulation time was recorded. In *A*, *C*–*E*, *G*, and *H*, the data are presented as mean  $\pm$  SEM; \* $p < 0.05$ , \*\* $p < 0.01$ , and n.s., no significant difference by student's *t* test. aPTT, activated Partial Thromboplastin Time; BDD, B-domain deleted; F8, factor VIII; flF8, full-length F8; HC, heavy chain; LC, light chain; LV, lentiviral vector; NC, negative control of F8 deficient plasma; PC, positive control of healthy donor plasma; qPCR, quantitative PCR; VCN, vector copy number; WB, Western blot.

transduced cells to determine vector copy number (VCN), and the values were normalized against cellular genome (Fig. 1C). Similar VCN in K562-flF8 and K562-F8-BDD cells was found, and the transgene mRNA expression was compared with house-keeping GAPDH mRNA based on RT-PCR and nucleic acid electrophoresis (Fig. 1D). The representative qRT-PCR result consistently showed that the F8-BDD expressed increased amount of mRNA as compared with the flF8.

The F8 protein expression was analyzed using an F8 ELISA kit and Western blot (WB) analysis. The results showed that the expression of F8-BDD in K562 S was 25-fold higher than that of flF8 (Fig. 1E). The WB detected full-length (170–200 kDa) and processed (80–90 kDa) products in the L, and 80 to 90 kDa and 43 kDa (A2 domain) products in the S from the K562-F8-BDD cells (Fig. 1F). Consistent with the mRNA levels, little to no F8-related proteins were detected in the K562-flF8 cells.

The F8 coagulation function was further analyzed based on activated Partial Thromboplastin Time (aPTT) assay using F8-deficient plasma. The latter was mixed with S from LV-transduced K562 culture. The results showed that K562-F8-BDD, but not K562-flF8, displayed therapeutic level of coagulation activities (Fig. 1G). Moreover, there were diverse patterns of clotting activities based on the coagulation assay, which illustrated that K562-flF8 showed flocculent precipitates, K562-F8-BDD showed clotted cementation, and the negative control K562 S showed no clotting activity (Fig. S1, A–C).

The F8-BDD produced higher amount of F8 proteins than flF8 in K562 cells and thus better clotting function, that is, shorter clotting time (Fig. 1G). However, when examined for the clotting function based on an equivalent amount of F8 protein (0.1 IU/ml) as measured by ELISA, the clotting time of flF8 per unit of protein was shorter than that of F8-BDD,

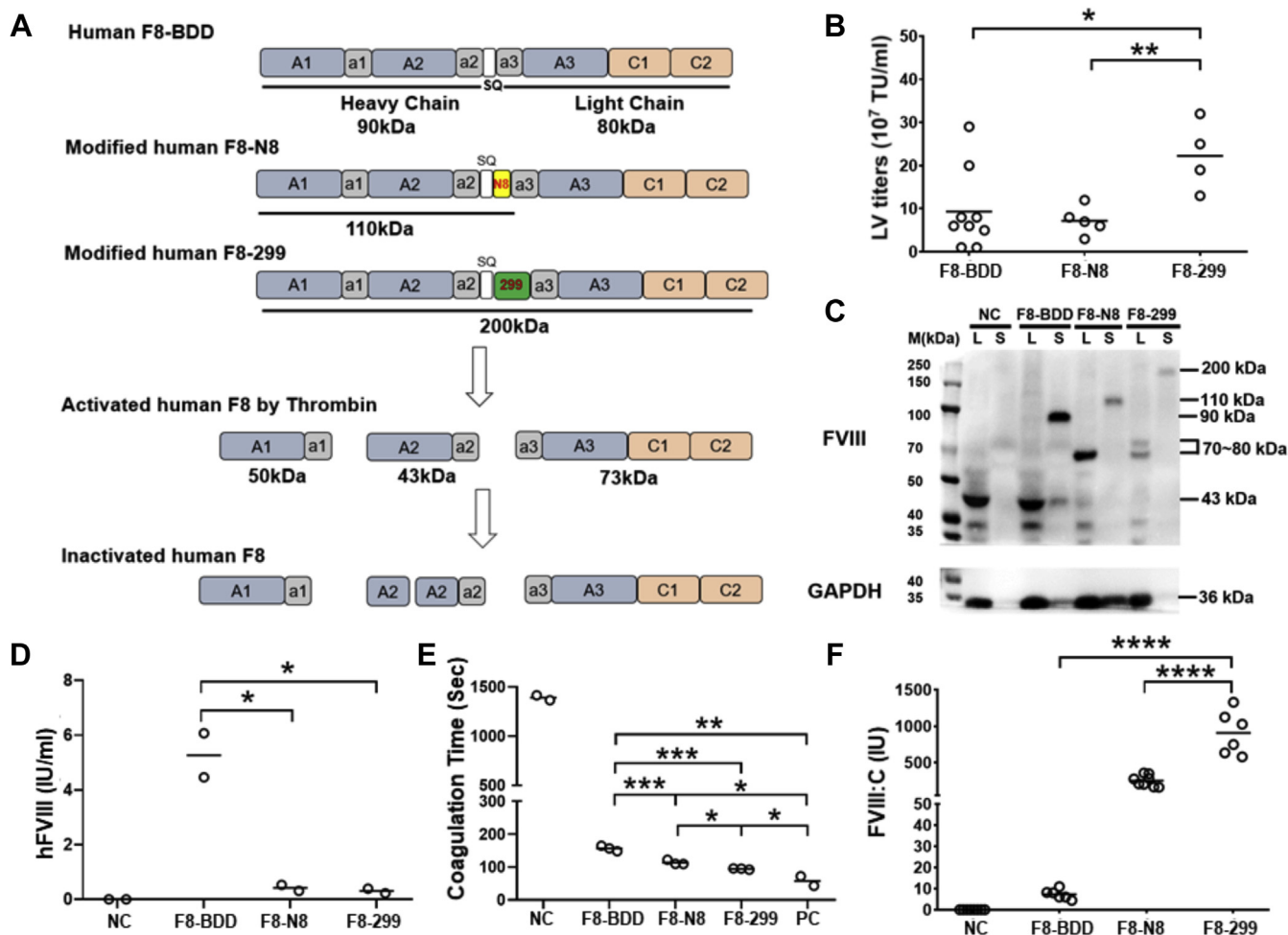


**Figure 2. Biochemical analysis of F8 expression and processing in LV-F8 modified ECs.** A, illustration of F8 activation and inactivation products of F8-BDD, F8-N8, and F8-299 with predicted molecular weights. B, comparison of vector titers of F8-BDD, F8-N8, and F8-299 constructs. C, WB analysis of F8 processing in LV-transduced ECs. The ECs were transduced with LV-F8-BDD, F8-N8, and F8-299 and the cell lysates and supernatants were analyzed by WB using a mouse anti-hFVIII mAb. D, determination of F8 protein concentration in F8-BDD, F8-N8, and F8-299 EA-hy926 cells using a human F8 ELISA kit. E, the F8 functional aPTT assay. The F8 deficient plasma was mixed with the supernatants of F8-BDD, F8-N8, and F8-299 EA-hy926 cells, and the coagulation time was compared. F, comparison of FVIII:C concentration ratios using the supernatants of F8-BDD, N8, and 299 EA-hy926 cells. The unit activity of F8, illustrated based on FVIII:C activity test, was determined by the F8 chromogenic assay. In B, D–F, the data are presented as mean  $\pm$  SEM. \* $p$  < 0.05, \*\* $p$  < 0.01, \*\*\* $p$  < 0.001, \*\*\*\* $p$  < 0.0001 by student's  $t$  test. aPTT, activated Partial Thromboplastin Time; BDD, B-domain deleted; EC, endothelial cells; F8, factor VIII; F8-N8, eight specific N-glycosylation sites; LV, lentiviral vector; WB, Western blot.

indicating that the flF8 had better biological activities than F8-BDD (Fig. 1H).

#### Decreased F8 protein expression but improved coagulation activities after B domain glycosylation modifications

The WB analysis suggested that the native B domain contained signals that could affect F8 processing, secretion, and function (Fig. 1). The intricate cell-dependent processing of F8 is critical to its activation and degradation. In plasma, the functional F8 exists as a heterodimer of a heavy chain (90-kDa) and a light chain (80-kDa) (13, 14). The unprocessed F8-BDD is around 170 kDa and is activated by thrombin cleavage to produce FVIIIa, which is released from von Willebrand Factor (vWF) as a heterotrimer composed of a 50 and a 43 kDa polypeptides derived from heavy chain, and a 73-kDa polypeptide derived from light chain (Fig. 2A) (14–17). When the A2 domain is degraded, F8 is inactivated. Importantly, the

heavily glycosylated B domain controls posttranslational modification of F8. With the goal of enhancing F8 secretion and function, we designed two novel F8 genes with increased glycosylation sites: the F8-BDD-N8 (F8-N8) by inserting eight additional native glycosylation sites and the F8-BDD-299 (F8-299) by restoring all of the glycosylation sites in the B domain. We constructed F8-N8 and -299 LVs and determined vector packaging efficiency and vector titer by qPCR. The F8-N8 modification decreased the LV packaging efficiency, whereas the F8-299 increased the packaging efficiency as compared with F8-BDD ( $p$  < 0.05) and -N8 ( $p$  < 0.01) (Fig. 2B).

To examine F8 processing and function, we transduced a human endothelial cell line (ECs), EA-hy926, at the same multiplicities of infection (MOI) of LV-F8-BDD, F8-N8, or F8-299, and examined VCN and F8 RNA expression. The results showed that all three LVs had similar transduction efficiencies and similar levels of RNA expression (Fig. S2, A–C). WB

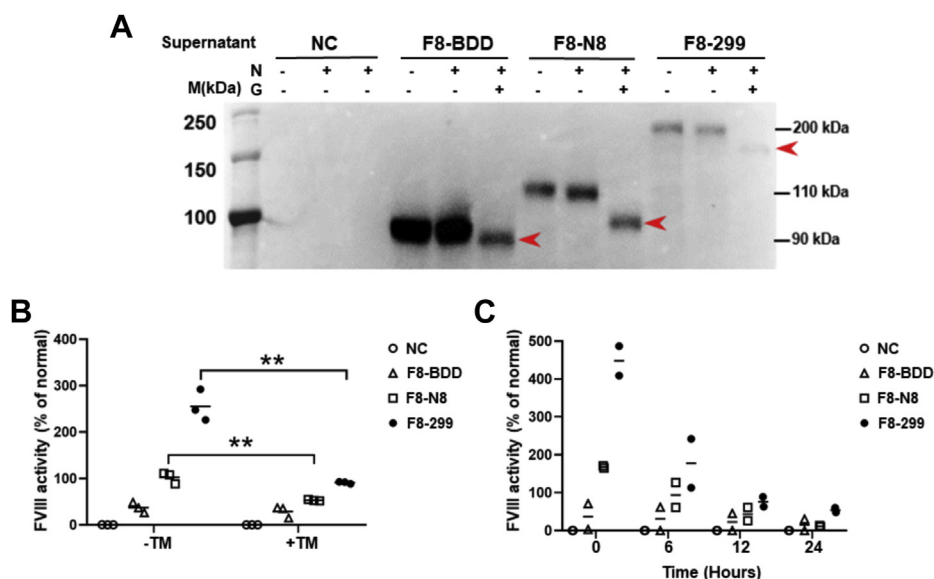


**Figure 3. Analysis of posttranslational F8 modifications and comparison of coagulation function.** *A*, deglycosylation treatment using neuraminidase (N) and peptide-N-Glycosidase F (G) to illustrate N-linked glycosylation. The arrowheads depict band shift after the inhibition of glycosylation. *B*, F8 functional analysis after inhibition of biosynthesis of N-linked oligosaccharides with tunicamycin (TM). The F8 activities were analyzed based on chromogenic assay after treatment with TM as indicated. \*\*\*\* $p < 0.0001$  by student's *t* test. *C*, analysis of F8 half-lives based on F8 chromogenic assay. In *B* and *C*, the data are presented as mean  $\pm$  SEM. BDD, B-domain deleted; F8, factor VIII; F8-N8, eight specific N-glycosylation sites; NC, negative control.

analysis of F8 in the L of the transduced cells revealed markedly increased intracellularly processed F8 to produce the inactive 43 kDa protein in both the native EA-hy926 cells (negative control) and the F8-BDD cells, but not the F8-N8 and F8-299 cells which accumulated more active forms of the 70 to 90 kDa products (L lanes, Fig. 2C). In the S, we detected increased sized F8 products from both F8-N8 and F8-299 cells (110 and 200 kDa, respectively), albeit at decreased amount, as compared with the ~100 kDa F8 protein in the F8-BDD cells (S lanes, Fig. 2C).

Quantitative ELISA showed higher levels of F8 expression (IU/ml) in the S of F8-BDD cells than the F8-N8 and F8-299 EA-hy926 cells (Fig. 2D). However, coagulation analyses based on aPTT assay (Fig. 2E) and chromogenic assay demonstrated significantly increased activities from both F8-N8 and F8-299 EA-hy926 cells, with the highest F8 activities detected in the F8-299 cells about 900-fold and 4-fold higher than that of F8-BDD and F8-N8 cells, respectively (Fig. 2F).

#### Increased F8 coagulation function and protein stability associated with restored B domain glycosylation

To examine N-glycosylation in F8, we treated the S from F8-BDD, F8-N8, and F8-299 EA-hy926 cells using glycosylation inhibitors, neuraminidase (N) and peptide-N-Glycosidase F (G), which induced deglycosylation and decreased molecular weights. The results showed evident size reduction in F8-N8 and F8-299 proteins after the inhibitor treatment (++ lanes *versus* -- lanes), but not for the F8-BDD protein (Fig. 3A). To further illustrate the importance of N-glycosylation in F8 function, we treated cells with tunicamycin (TM), which blocks the first step in the biosynthesis of N-linked oligosaccharides in cells. In all three LV-transduced cells, we observed decreased F8 activities after the TM treatment, significantly

more so in the F8-N8 and F8-299 cells ( $p < 0.01$ ), supporting the importance of full glycosylation restoration in functional F8 secretion (Fig. 3B). We further examined the effect of glycosylation on the half-life of the F8 protein. The results showed that the F8 activities decreased by almost half after 6 h, which is consistent with the reported half-life of F8 protein (Fig. 3C). Interestingly, F8-299 maintained higher F8 activities at all times, with residual activities remained after 24 h, suggesting increased stability of the F8-299 protein.

#### Enhanced procoagulation cofactor interactions after restoration of F8 B domain glycosylation

To investigate whether the B domain interacts with procoagulation cofactors, we treated the S of the transduced cells with vWF and thrombin (FIIa). The addition of thrombin enhanced F8 activation and produced more A2-related 43 kDa protein (Fig. 4A), which was associated with an increase in F8 activities as illustrated by functional assay performed at 2-min intervals (Fig. 4B); the F8 activity increased slowly in the F8-BDD and F8-N8 S but rapidly in the F8-299 S. We postulated that there was more F8 hydrolyzation by thrombin in the F8-299 S. The cofactor vWF (~100 kDa) was associated with F8, and using antibody to vWF, we detected higher amount of vWF in the L of F8-N8 and F8-299, but much less in the F8-BDD L by WB (Fig. 4C; the same blot as Fig. 2C but stripped off human F8 (hF8) Ab and re-probed with vWF Ab). We further examined the association of F8 with vWF through coimmunoprecipitation (coIP) using F8 antibody to precipitate vWF protein and vWF antibody to develop the WB. The results illustrated a trend of increased association of F8 with vWF in the F8-N8 and F8-299 L as compared with the F8-BDD L (Fig. 4D).

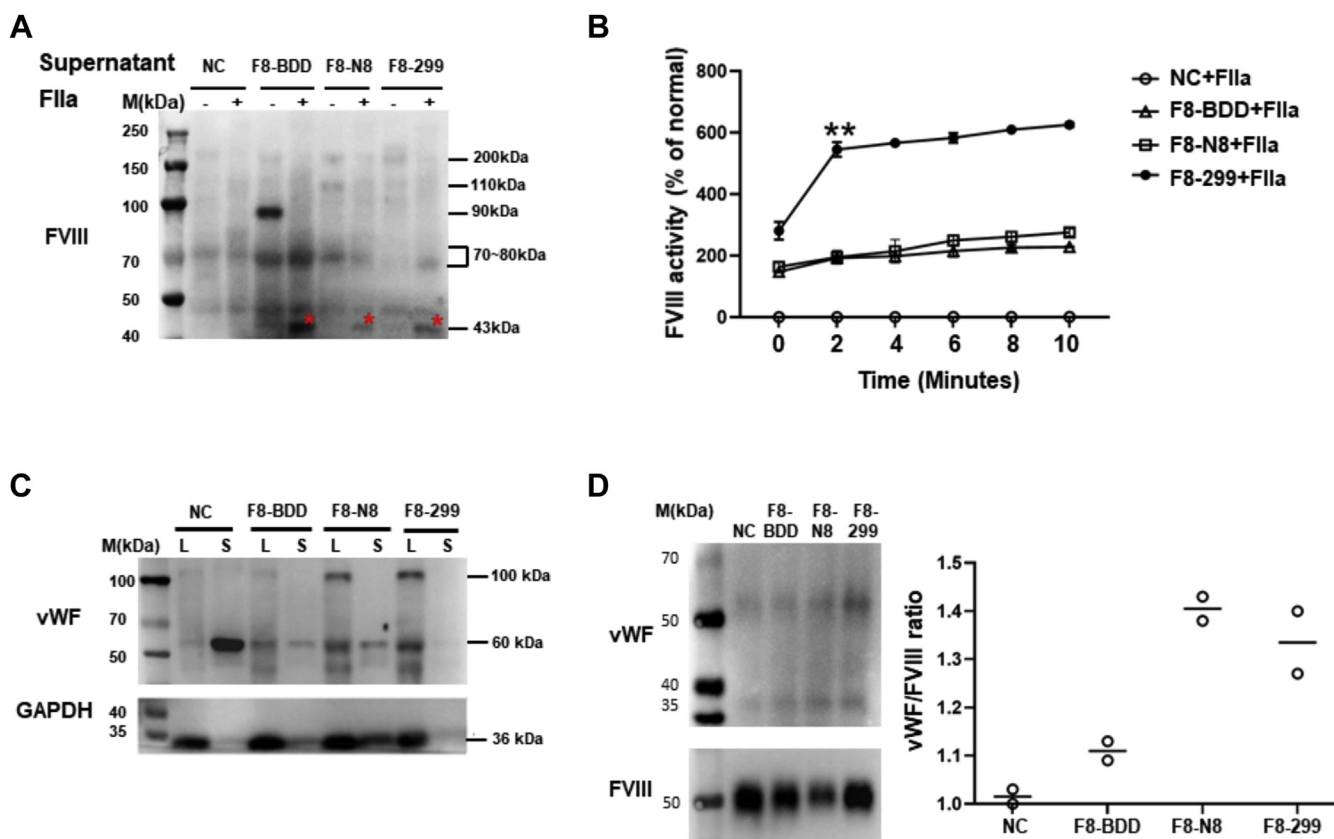


**Figure 4. Analysis of F8 cofactor correlations in the coagulation process.** A, F8 before and after activation by thrombin (FIIa) analyzed using SDS/PAGE. The asterisks depict the 43-kDa cleaved inactivation product of F8 protein. B, the kinetics of F8 activities after adding the FIIa cofactor to the supernatants;  $**p < 0.01$  by student's *t* test. C, WB analysis of vWF protein processing in LV transduced ECs with a polyclonal anti-rabbit Ab. This was the same blot as Figure 2C but stripped off the hF8 Ab and reprobed with vWF Ab. The lysates of EA-hy926-F8-N8 and F8-299 cells showed ~100-kDa bands as the cleaved products of vWF. D, CoIP using protein A/S beads with F8 Ab to capture vWF in the F8-vWF complex. The F8 protein and the coIP vWF were detected by WB using anti-FVIII and anti-vWF Abs. The ratios of vWF/F8 were determined based on chromogenic intensities read with ChemiDoc Touch. In B and D, the data are presented as mean  $\pm$  SEM. Ab, antibody; BDD, B-domain deleted; coIP, coimmunoprecipitation; ECs, endothelial cells; F8, factor VIII; F8-N8, eight specific N-glycosylation sites; hF8, human F8; LV, lentiviral vector; NC, negative control; vWF, von Willebrand factor; WB, Western blot.

#### Functional analyses of LV-F8-BDD, F8-N8, and F8-299 in HA mice

*In vitro* assays supported improved coagulation activities of the modified F8 proteins. We next tested these LV-F8 vectors in an F8-knockout mouse model (HA mice). The Lin-murine (m) HSCs were isolated from bone marrow (BM) of the HA mice and transduced with LV-F8-BDD, F8-N8, or F8-299 ( $n = 5$  each) for transplantation, as illustrated in Figure 5A. After myeloablation, each of the HA mice received  $5 \times 10^5$  Lin-cells through tail vein infusion at day 0. Genomic DNA qPCR analysis detected similar VCNs in the transduced mHSCs (~10–20% transduction rate, Fig. 5B). The hF8 expression in the plasma was measured using a hF8-specific ELISA kit 2 weeks after HSC transplantation (HSCT). We detected hF8 levels at ~1 IU/ml for the F8-299 recipients and 0.1 and 0.5 IU/ml for the F8-BDD and -N8 recipients, respectively ( $p < 0.0001$  and  $p < 0.01$ , Fig. 5C). Besides high circulating hF8, the F8 activity in the F8-299 recipients increased over time from 5% to 8% and remained stable for 8 weeks in the plasma, which was substantially higher than that of the F8-BDD and F8-N8 recipients (Fig. 5D). Flow cytometry analysis of intracellular hF8 in blood mononuclear cells using anti-hF8 antibody showed 71.46%, 52.16%, and 43.75% of F8 positive cells

in F8-299, F8-N8, and F8-BDD recipients, respectively (Fig. 5E).

To examine the bleeding phenotype, the HA mice were subjected to bleeding diathesis test by tail clipping 8 weeks after HSCT, and the results showed markedly decreased bleeding levels in F8-N8 and F8-299 transplanted mice as compared with the mock HA mice (Fig. S3). The concentration of hemoglobin (Hb) in the blood is in reverse correlation with bleeding, and increased bleeding leads to reduced Hb levels. Thus, we examined Hb in the blood and found the lowest level of Hb in the F8-299 recipients than the F8-BDD and F8-N8 mice (Fig. 5F). The bleeding time of the F8-299 recipients was similar to the WT mice in repeated tests (Fig. 5G), and the bleeding time did not differ significantly between the F8-BDD and F8-N8 recipients ( $p = 0.22$ ). These results confirmed that the clotting function was nearly fully restored in the F8-299 treated HA mice.

#### F8 antibody response in F8-BDD, F8-N8, and F8-299 LV-mHSC-transplanted HA mice

Immune inhibitor affecting HA treatment is a critical issue in F8 therapy. To evaluate the immune response after LV gene

## Improved lentiviral FVIII gene therapy

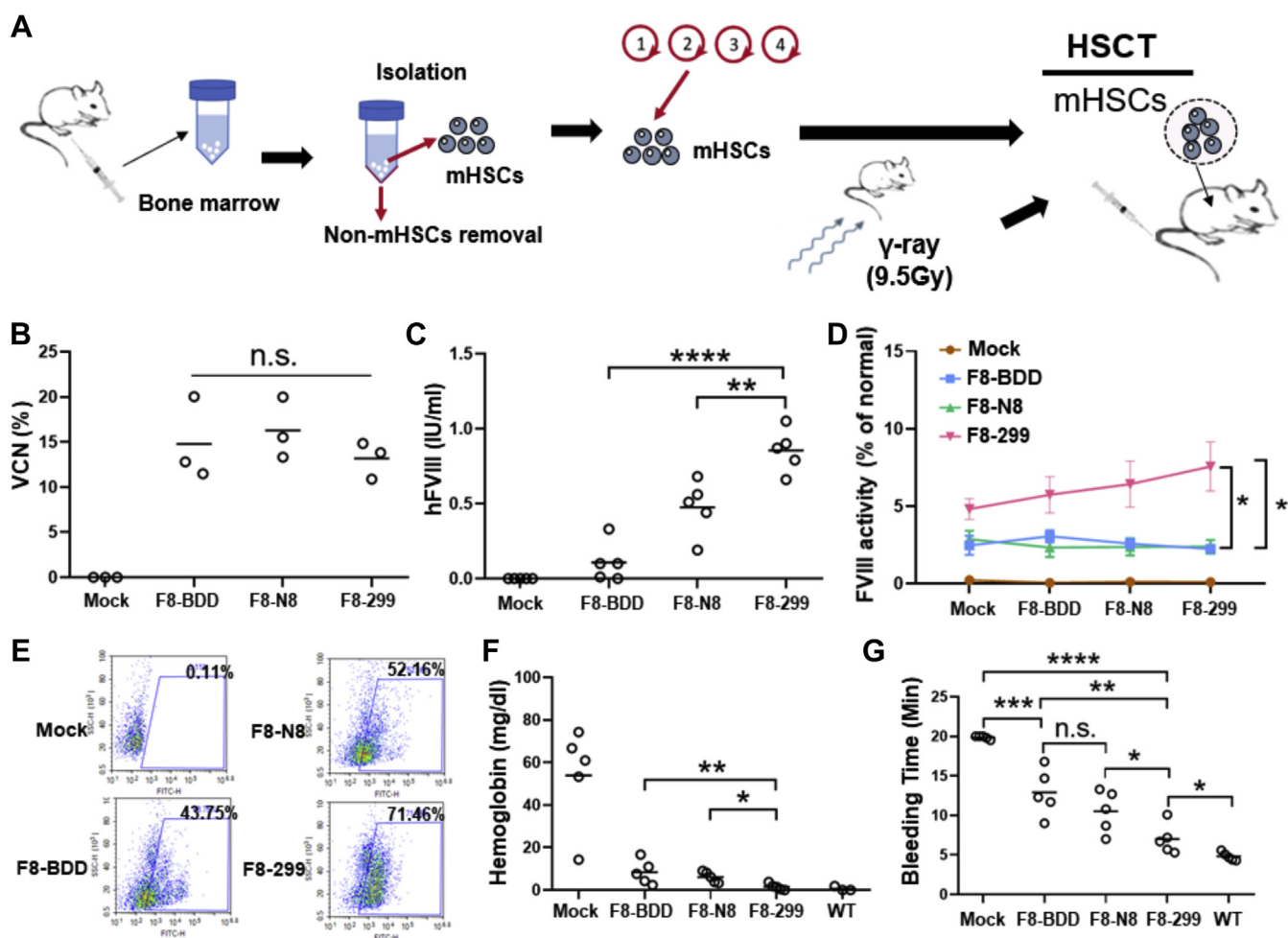


**Figure 5. Functional analyses of LV-F8-BDD, F8-N8, and F8-299 in HA mice.** A, schematic illustration of BM transplantation of HA mice using mHSCs transduced with LV-F8-BDD, -F8-N8, or -F8-299. B, determination of transduction efficiency and VCN of mHSCs using gDNA qPCR. C, expression of hF8 levels in the plasma 4 weeks after transplantation using a human F8 ELISA kit. D, kinetics of F8 activities by chromogenic assay. E, detection of intracellular hF8 expression in blood cells by flow cytometry 4 weeks after transplantation. F, analysis of hemoglobin concentration (mean  $\pm$  SEM) in blood 8 weeks after transplantation by measuring the absorbance at 575 nm of the plasma. G, tail bleeding time analysis (mean  $\pm$  SEM) assessed by monitoring the blood flow into collection tubes containing saline solution. The time required to stop bleeding was recorded and plotted. In B–D, F, and G, the data are presented as mean  $\pm$  SEM. \* $p$  < 0.05, \*\* $p$  < 0.01, \*\*\* $p$  < 0.001, \*\*\*\* $p$  < 0.0001. n.s., no significant difference by student's  $t$  test. BDD, B-domain deleted; BM, bone marrow; F8, factor VIII; F8-N8, eight specific N-glycosylation sites; gDNA, genomic DNA; HA, hemophilia A; hF8, human F8; LV, lentiviral vector; mHSCs, murine/mouse hematopoietic stem cells; qPCR, quantitative PCR; VCN, vector copy number.

therapy, we examined VCN by qPCR in the heart, lung, liver, spleen, kidney, and testis of the transplanted HA mice. We detected ~1 to 5 % LV-transduced cells in the liver, spleen, and kidney, and no LV DNA was detected in the heart, lung, and testis (Fig. 6A). In addition, LV DNA was examined in the blood 8 weeks after transplantation, and higher VCN was detected in F8-299 (~2%) than F8-BDD and F8-N8 recipients (Fig. 6B).

Intracellular flow cytometry analyses of hF8 in different hematopoietic lineages of the F8-299 mice illustrated that no hF8-positive myeloid cells (CD11b+) and macrophages (F4/80+) were detected in the liver and spleen. Similar results were obtained for the F8-BDD and F8-N8 mice (Fig. S4). Only 20 to 60% ( $n = 3$ ) hF8-positive cells were consistently detected in megakaryocytes (CD41+) and ECs (KDR and CD31 positive) in the spleen (Fig. 6C). F8-specific antibody formation in the plasma after transplantation was examined at various time points based on Bethesda assay, referred to as inhibitor titer.

The results showed little to no inhibitor formation or production of F8-specific IgG in the F8-299 recipients, but strong inhibitor reaction was detected in the F8-BDD and F8-N8 recipients. (Fig. 6, D and E).

## Discussion

The current treatment for hemophilia involves costly and painful life-time PRT. A one-time solution such as gene therapy is highly demanded. In particular, even modest amount of F8 or F9 delivered by gene therapy can ameliorate bleeding in affected individuals.

Adeno-associated virus vector (AAV)-mediated hemophilia gene therapy has reported encouraging results in a number of studies, and many are in phase II/III clinical trials, approaching the stage of final product approval (18). However, disadvantages such as preexisting antibody response to AAV, the high immunogenicity of the AAV capsid protein, diminished

expression and potential liver injury, and the extremely high production cost of AAV vectors present major limitations.

LV-mediated hemophilia gene therapy has been in preclinical and early clinical research (19, 20). A large number of animal studies and clinical reports support that LV displays stable and sustained gene expression feature with low immunogenicity. Because of the limited payload of the AAV vectors, flF8 gene can only be inserted into LV. To overcome the size limitation, truncation of F8 gene without affecting its function has been widely applied, mainly referring to as the F8-BDD strategy (21, 22).

The packaging efficiency of LV is determined by many factors, including the size of the insert and the specific nucleotide sequence. We found that the F8-gene size reduction increased LV packaging efficiency; the titer of LV-F8-BDD was 100 times higher than that of the LV-flF8 (Fig. 1A). However, although F8-BDD is the favored F8 gene therapy configuration under the premise of the same protein amount, the coagulation function of F8-BDD is not as effective as that of flF8, which was demonstrated in Figure 1, F and G, suggesting that the B domain of F8 may play an important role in F8 biosynthesis.

The F8 coagulation function requires many post-translational modifications and cofactor interactions, which has not been clearly deciphered. The F8 expression and secretion involve both mRNA stability and protein transport from ER to the Golgi apparatus. The ER chaperones promote Golgi transport *via* interactions with LMAN1 protein, which facilitates posttranslational addition of N-chain oligosaccharide residues. To enhance ER-Golgi transport of F8, N-glycosylation modification in the B domain has been attempted (8, 23, 24), but here, we incorporated a synthetic multi-N-glycosylation sites in F8-N8 and a full restoration of N-glycosylation in F8-299. We conducted a detailed biochemical analysis of F8 protein processing after B domain

modifications. It is important to point out that different from many F8 studies, the use of ECs in this study as the F8-processing machinery might have greatly facilitated the characterization of the posttranslational mechanics of F8 biosynthesis. According to WB patterns in Figure 2C, it was evident that F8-299 increased the posttranslational modification of F8 protein, which slowed down the process of protein synthesis and resulted in an increase in the secretion of an unprocessed protein. The results showed that glycosylations affected the integrity of F8 protein secretion and coagulation function.

In the coagulation pathway, FVIIIa, as a cofactor of activated-factor IX, cocatalyzes activated factor X, and activates Factor II to stimulate the coagulation cascade (25–28). The activated FII is also one of the inactivation partners of F8. On the other hand, vWF, another essential cofactor, promotes F8 secretion. F8 and vWF are synthesized and stored together in granules in cell bodies such as platelets and ECs and can be released together in response to a proper agonist, such as 1-desamino-8-D-arginine vasopressin of ECs (10). It has been observed that F8 is associated with vWF when secreted from ECs *in vitro*. This suggests that the function of F8 is modulated through cofactor interactions and highly related to the post-translationally modified secreted forms.

Although the liver, and in particular liver sinusoidal ECs (LSECs; lymphatic endothelial and hematopoietic cells), are considered the main source of F8 biosynthesis (29–32). F8 synthesizes in other tissues and cell types, such as the spleen and myeloid cells, have been reported (33–37). Recent studies have presented evidence that ECs are the main or even the only source of *de novo* F8 biosynthesis, and F8 activation preferentially occurs in ECs and hematopoietic cells, rather than in hepatocytes (38–40). Therefore, ECs and hematopoietic cells may represent the *bona fide* physiological location for F8 biosynthesis. In many aspects, ECs closely interact with HSCs.

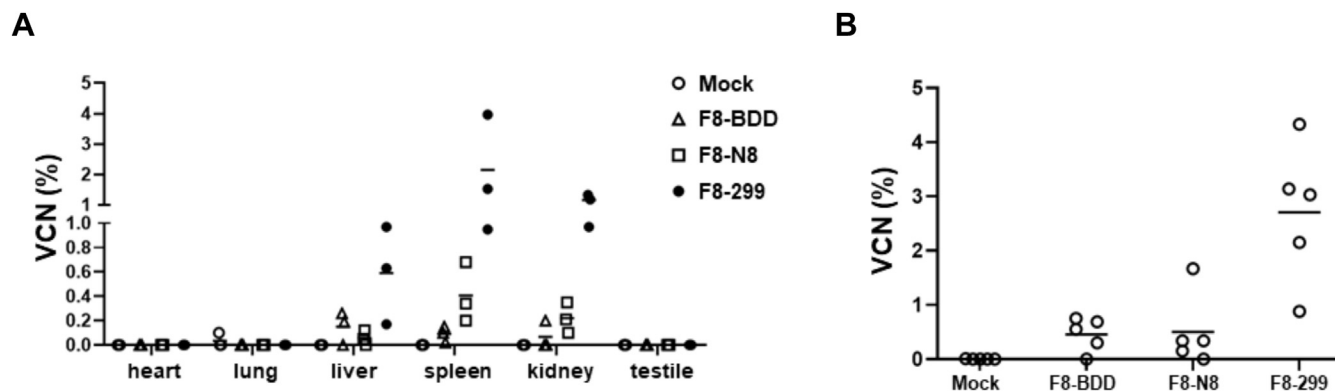


**Figure 6. Anti-hF8 response in F8-BDD, F8-N8, and F8-299 mHSC-treated HA mice.** A and B, VCNs in the depicted organs (A) and blood (B) from the LV-F8 transplanted HA mice. The F8-299 recipients showed the highest hF8 LV DNA in all of the examined sites. C, biodistribution of hF8 in different cell lineages in liver and spleen by flow cytometry. The cells were collected from the livers and spleens of mock and F8-299 treated mice and stained with anti-hF8 Ab *via* intracellular staining, as well as cell surface marker for myeloid marker (CD11b), megakaryocyte marker (CD41), macrophage marker (F4/80), and EC markers (KDR and CD31) 60 days after mHSC. D, analysis of inhibitor titer kinetics using plasma from transplanted HA mice. The plasma was collected at various time points, and the inhibitor titer (BU) was determined based on a modified Bethesda assay. E, determination of anti-hF8 IgG levels by ELISA in the transplanted HA mice. The plasma of transplanted mice was collected 60 days after transplantation and diluted at 1:200 to determine anti-hF8 levels. In A, B, D, and E, the data are presented as mean  $\pm$  SEM. \*\*\* $p$  < 0.001 by student's  $t$  test. Ab, antibody; BDD, B-domain deleted; EC, endothelial cells; F8, factor VIII; F8-N8, eight specific N-glycosylation sites; HA, hemophilia A; hF8, human F8; HSCT, HSC transplantation; LV, lentiviral vector; mHSC, murine hematopoietic stem cell; VCNs, vector copy numbers.

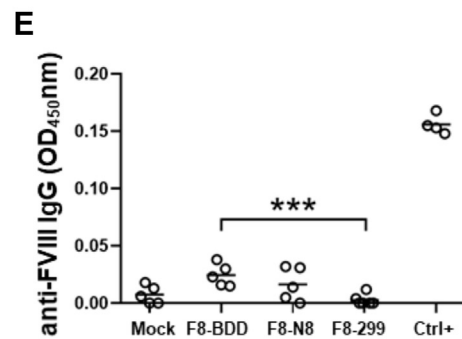
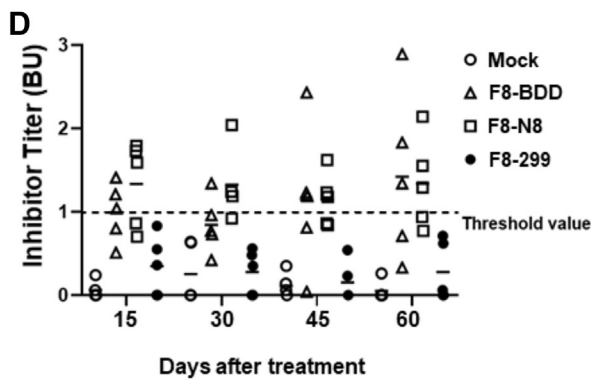
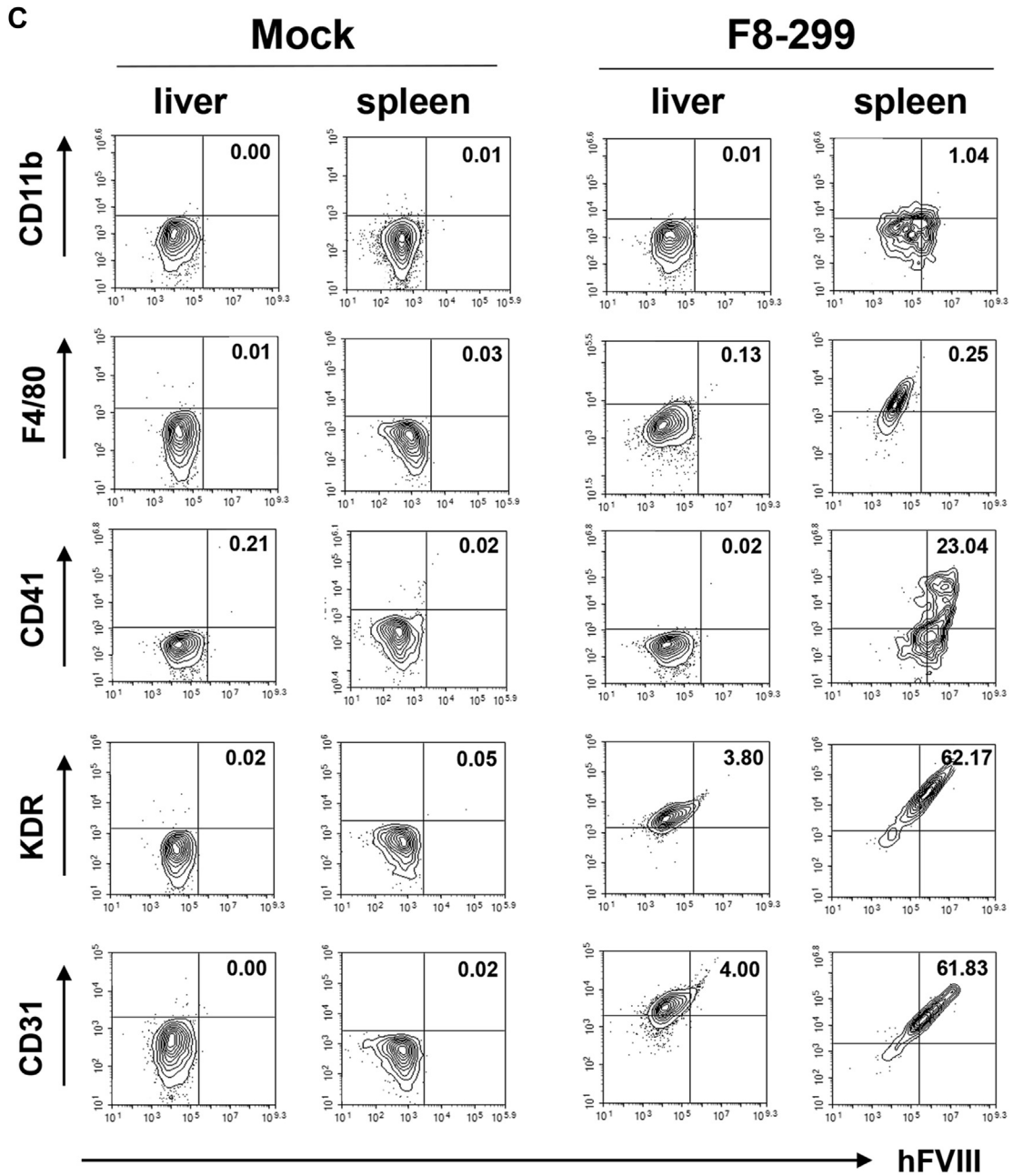


Figure 6. (continued).

The main source of ECs is peripheral blood outgrowth ECs, which is a class of endothelial progenitor cells generated in the BM and then enter the peripheral circulation, expressing CD31 and CD34 (41). Therefore, HSCs are considered ideal cellular targets for HA gene therapy, not only because they can self renew and secrete the therapeutic molecules directly into the bloodstream, but also that HSC gene transfer may establish immune tolerance or nonresponsiveness to the therapeutic proteins, which makes LV auto-HSCT gene therapy an attractive gene therapy strategy for HA. Novel direct-targeted delivery of HA gene vectors into particular tissues using tissue-specific promoters to reduce ectopic expression and antibody formation could improve the efficacy and safety and reduce the cost without *ex vivo* cell processing (42–44).

Studies of F8 knockout mice revealed that the F8-299 recipients exhibited a better therapeutic effect than the F8-BDD and F8-N8 recipients at the same HSCT gene transfer rate. We demonstrated that the F8 gene expression was enhanced through the use of a strong universal promoter and codon-optimization, but the mere increase in F8-BDD expression resulted in low-clotting activity accompanied by a strong inhibitory response. The biochemical analyses of F8 glycosylation and cofactor interactions emphasized the importance of a balanced posttranslational biosynthesis of the F8 protein in modulating its clotting function. Nevertheless, future human trials are necessary to elucidate the long-term therapeutic efficacy of these novel F8 variants.

In conclusion, the F8-299 variant not only maintained the size-reduced F8 transgene feature with high LV packaging efficiency, but also displayed a reduced protein level yet retained an increased functionality and serum stability of the F8 subunits, which resulted in correction of the genetic defect, making it a major step forward in improving HA gene therapy strategy.

## Experimental procedures

### F8-BDD modification

The codon-optimized flF8 gene was constructed by cloning the hF8 cDNA into the LV-expression vector (45). The F8-BDD construct was created by modifying the hF8 cDNA using synthetic codon-optimized BDD fragment between the A2 and A3 domains (46). The two modified F8-BDD cDNA sequences were also codon-optimized, chemically synthesized, and cloned into the LV. The F8-N8 included the 54 aa containing eight putative glycosylation sites, and the F8-299 included all 299 aa of the B domain, which were sequence verified.

### LV construction and production

LVs were generated using the NHP/TYF-derived pEGWI LV system, as described previously (47, 48). F8-BDD, F8-N8, and F8-299 cDNAs were cloned into this vector behind the human EF1 $\alpha$  promoter. Selectively cloned HEK-293T cells were transfected for vector production. The LVs were prepared and concentrated, as previously described (49, 50).

### Cell cultures

The K562 myeloid and EA-hy926EC lines were obtained from ATCC and cultured in RPMI and Dulbecco's modified Eagle's medium (DMEM) (Hyclone), respectively, supplemented with 10% fetal bovine serum, and 1% penicillin/streptomycin. All the cells were cultured at 37 °C in 5% CO<sub>2</sub> incubators.

### LV transduction

K562 cells were transduced with LVs at MOI 100 by incubating approximately  $1 \times 10^4$  cells with LV in a final volume of 600  $\mu$ l medium, supplemented with polybrene (8  $\mu$ g/ml; Sigma-Aldrich), and centrifuged at 100g for 100 min. The EA-hy926 cells were plated at  $4 \times 10^4$  per well in 6-well plates (CORNING), and after 18 h incubation, the cells were transduced with LV at MOI 50 in 600  $\mu$ l medium supplemented with polybrene, as described. After 24 h, the cell media were changed to serum-free media. After a further 72 h, the S and cell lysates were collected, and the S were concentrated with 30 Kd ultrafiltration centrifuge tubes.

### Determination of VCN in transduced cells

The LV VCN in the transduced cells or tissues was determined by quantitative SYBR green real-time qPCR. gDNA was harvested from the cells or tissues using a gDNA purification kit (Promega Corp). The sequences for LV and GAPDH gene primers are as following: LV forward primer: 5'-GGGACTT-GAAAGCGAAAGTAAAG-3', reverse primer: 5'-TTTGCGTACTCTGCAGTC-3'; GAPDH forward primer: 5'-ACATCGCTCAGACACCATG-3', reverse primer: 5'-TGTAGTTGAGGTCAATGAAGGG -3'. Amplification was done in triplicate reactions, which consisted of 1  $\mu$ l template, 12.5  $\mu$ l 2 $\times$  SYBR green qPCR master mix, and determined optimal primer concentration. The optimized primer concentrations used in qPCR reactions were determined to be 500 nM for each primer for LV and GAPDH, 300 nM for each primer for LV, and 100 nM of each primer for GAPDH. The condition for the PCR was as suggested by BioRad using the CFX96Touch qPCR system (BioRad) at 95 °C for 10 min, followed by 40 cycles of 95 °C for 30 s, 60 °C for 30 s, and a dissociation curve analysis to confirm amplification of a single amplicon. The CT value  $\geq 37$  were considered as an undetectable value. The LV VCN was calculated based on the  $2^{-\Delta\Delta C_t}$  method and normalized against the GAPDH genome copies to determine VCN per cell or per  $\mu$ g gDNA.

### Animal procedures

All mouse protocols were reviewed and approved by the institutional animal case and use committee at Shenzhen Geno-Immune Medical Institute. The F8-knockout HA mice of C57BL/6 background, purchased from Biosubstrate Technologies were used in all experiments. All the mice were housed under pathogen-free conditions, and 5- to 6-week-old male HA mice were conditioned with 950 cGy using an X-ray irradiator (Faxitron). The transplantation was performed 4 days after irradiation *via* tail vein injection. The mice were

## Improved lentiviral FVIII gene therapy

sacrificed 64 days after transplantation, and the organs were harvested and kept in  $-80^{\circ}\text{C}$  until use. Prebleeding was performed by tail-clipping followed by electrocautery. After the vector injection, the mice were bled by retro-orbital bleeding procedure. Plasma was frozen immediately and stored at  $-80^{\circ}\text{C}$  until use.

### mHSC transduction and transplantation

To isolate mouse HSCs (lineage negative cells, Lin<sup>-</sup>), the BM of 6- to 8-week-old mice was flushed from femurs and tibiae. The Lin<sup>-</sup> cells were obtained by immunomagnetic negative selection from the total BM cells, using a mouse hematopoietic progenitor cell isolation kit (STEMCELL Technologies), and cultured at a density of  $1 \times 10^6/\text{ml}$  in Stem-Span medium (Lonza) supplemented with cytokines including recombinant mouse stem cell factor, mouse FMS-like tyrosine kinase 3-ligand, mouse thrombopoietin, and mouse interleukin-6. The Lin<sup>-</sup> cells were transduced with LVs at MOI 40. After transduction, the Lin<sup>-</sup> cells were diluted in PBS to a total volume of 200  $\mu\text{l}$  and infused *via* tail vein into mice.

### Analysis of LV-F8 RNA expression

The RNA was harvested from transduced cells using an RNA purification kit (Promega Corp). Approximately, 200 ng of RNA was reverse-transcribed into cDNA using a two-step HiScript III RT SuperMix kit (Vazyme). RT-PCR was performed at  $37^{\circ}\text{C}$  for 15 min and  $85^{\circ}\text{C}$  for 5 s. The F8 and human GAPDH primers were used for PCR (see Table S1). The cDNA produced was separated on a 2% agarose gel by electrophoresis. PCR amplification was carried out using 2 $\times$  Taq Master Mix (Vazyme Biotech Co, Ltd) in a T100 Thermal Cycler PCR (Bio-Rad). The PCR products were resolved on a 2% agarose gel (BG-Power 300, BayGene biotech). The gel was exposed and analyzed using a ChemiDoc Touch imaging system (Bio-Rad).

### WB analysis

For WB analysis,  $1 \times 10^6$  cells were seeded into the six-well plate with 1.5 ml medium. After cell adherence, the medium was replaced with 1 ml serum-free medium (Freestyle, Gibco; Invitrogen). The S and cultured cells (L) were collected after 72 h. The cells were washed with cold PBS three times and then treated with ice cold RIPA buffer (Vazyme), supplemented with protease inhibitor mixture (Boster Biological Technology) and incubated at  $4^{\circ}\text{C}$  for 30 min. The S were concentrated using 30 kDa ultrafiltration tubes. The protein concentration was determined by BCA protein Assay (Thermo Fisher Scientific). Equivalent protein was boiled for 5 min, separated in a 7.5% SDS polyacrylamide gel, and then transferred to PVDF membrane (Bio-Rad). The membrane was blocked with 5% BSA buffer (Biofrox, 4240GR100) at room temperature for 1 h. The membrane was then incubated with primary antibody (F8: 1:500, sc-73597, Santa Cruz Biotechnology; vWF: 1:1000, ab6994, Abcam; GAPDH: 1:5000, #5174, Cell Signaling Inc) overnight at  $4^{\circ}\text{C}$ . After three washes, the

membranes were incubated with 1:5000 dilutions of horseradish peroxidase-conjugated secondary anti-mouse or -rabbit antibody (#91196, #7074, Cell Signaling Inc) for 1 h. The signals were detected with an enhanced chemiluminescence kit (ECL, Bio-Rad) and exposed and analyzed under the ChemiDoc Touch imaging system.

### The vWF and F8 protein coimmunoprecipitation

The F8 monoclonal antibody (mAb) was added to culture S for antigen (Ag)-antibody (Ab) binding and mixed on a horizontal shaker at  $4^{\circ}\text{C}$  overnight. The protein A/G PLUS-agarose beads (Santa Cruz Biotechnology) were added to the Ag-Ab complex at a volume ratio of 1:100 on a rotating shaker for 30 min, and the beads were collected in a centrifuge at 14,000g at  $4^{\circ}\text{C}$  for 1 min. The beads were resuspended and washed with 1 ml buffer and centrifuge for 1 min to collect the binding products, and this was repeated twice. The coIP pellets were then analyzed by WB using anti-vWF and anti-FVIII Abs.

### Quantitative assessment of hFVIII expression

The concentration of F8 protein in S was determined using a human F8 ELISA kit (Abcam), as per manufacturer's instruction. The samples were diluted at 1:100 in sample diluent provided and analyzed in duplicates. The standard curves of hF8 were generated according to the dilution instructions, and the optical density was read using a Cytation Hybrid Multi-Mode Reader (BioTek). The unit for F8 is shown as IU/ml.

### Detection of anti-FVIII antibodies in the HA mice

ELISA on plasma from LV-treated mice was performed to detect anti-FVIII Abs, as described (51). The titer of the inhibitory Abs was determined using the modified Bethesda method. Briefly, the plasma samples from transplantation recipients after 60 days were mixed with 2  $\mu\text{l}$  normal human plasma. A standard curve was plotted according to the amount of plasma added, as shown in Table S2. Following incubation at  $37^{\circ}\text{C}$  for 2 h, the residual F8 activity was determined using a 1-step aPTT assay. One Bethesda unit was defined as the reciprocal of the dilution of test plasma at which 50% of hF8 activity was inhibited. The sensitivity of the assay was at 1 Bethesda unit/ml.

### The in vitro and in vivo F8 activity assays

The *in vitro* assay for F8 activity was done using the aPTT assay and two-step coagulation assay (chromogenic assay, HYPHEN BioMed, FR), and the *in vivo* assay was done using two-step coagulation and tail clip assays. The calibration was performed using a normal pooled citrated plasma. The results were expressed as a percentage of correction. *In vitro* clotting time is capped at 40 min. FVIII:C is the ratio of F8 activity detected by chromogenic assay to the Ag of F8. The tail clip assay was performed with modifications from a previously described protocol (52). The entire distal portion of the tail was cut off (diameter, 2–2.5 mm) from anesthetized mice 60 days after transplantation. The bleeding was

recorded in a 40 ml saline solution tube for 20 min. The precipitated red blood cells were treated using a hemoglobin colorimetric assay kit (Biovision) and red blood cell lysis buffer (BD Biosciences), and the absorbance was measured at 575 nm using a Bio-Tek Cytation 5 Cell Imaging Multi-Mode Reader (Bio-Tek). The results were analyzed by comparing the LV-treated HA mice with WT and untreated HA mice.

### Cell preparation and flow cytometry

For analysis of cell-surface markers by flow cytometry, the plasma, liver, or spleen cells were incubated with normal rat serum at 4 °C for 30 min and then stained with goat anti-human F8 Ab (Santa Cruz Biotechnology) or isotype Ab control (purified mouse IgG2 $\alpha$ , BD Biosciences) in FACS buffer at 4 °C for 30 min. After washed with PBS, the samples were stained with a secondary goat anti-mouse IgG (H + L) directly conjugated with Alexa Fluor-488 (Invitrogen) in FACS buffer for 30 min. The plasma collected from HA mice were used as controls. For intracellular staining, the cells were permeabilized using 0.1% Triton X-100 in PBS for 10 min and blocked with 3% BSA in PBS at room temperature for 1 h. The staining was performed using primary Abs against F8 (Santa Cruz Biotechnology, 1:50 dilution) at room temperature for 1 h. After PBS washing three times, the cells were stained with a secondary anti-mouse Ab conjugated at room temperature in the dark for 30 min.

The liver cells were isolated from the mice and treated with collagenase, as previously described (53). The spleens and lymph nodes were homogenized, and the single cell suspensions were prepared after lysis with red blood cell lysis buffer (BD Biosciences). The antibodies used for surface and intracellular staining were as following: PE-Cy7 rat Anti-CD11b (clone M1/70), PE anti-mouse CD41 (clone MWReg30), anti-rat F4/80 mAb (eBioscience), anti-mouse CD31 mAb (Invitrogen), and anti-rabbit VEGF receptor 2 mAb (Invitrogen). The secondary Abs and the isotype-control Abs used to determine nonspecific background signal included Alexa Fluor 488 goat anti-rat IgG (H + L), Alexa Fluor 488 goat anti-mouse IgG (H + L), and Alexa Fluor 488 goat anti-rabbit IgG (H + L) (Invitrogen). The analyses were performed using a NovoCyte Quanteon flow cytometer (ACEA Biosciences) and data analyzed using the ACEA NovoExpress software.

### Statistical analysis

Statistical analysis was performed by applying the Wilcoxon matched-pairs signed-rank test using GraphPad Prism 8 software (GraphPad Inc). All the data were presented as mean  $\pm$  SEM. Statistical significance of differences between groups was evaluated using Student's *t* test or ANOVA one-way test (Tukey) and specified as \**p* < 0.05; \*\**p* < 0.01; \*\*\**p* < 0.001; \*\*\*\**p* < 0.0001; n.s., no significant difference.

### Data availability

All raw data used for figure generation in this study can be obtained by contacting the corresponding author.

*Supporting information*—This article contains supporting information.

*Acknowledgments*—We thank Haokun Yuan and Haolin Wang for caring for the mice, Yue Qin for the LV packaging, Liu Xu for qPCR detection, Ying Shi for advice of experimental methods, and Dr Biljana Horn and Thomas Horn for reading and revising the article. This work was supported by grants from the Foundation for Introduction and Training of Outstanding Scholarship of the National “985” Project, China (A1098531023601102) and the Fundamental Research Funds for the Central Universities, China (ZYGX2016Z009).

*Author contributions*—J. G. and L.-J. C. investigation; J. G., T.-H. C., J. Z., H. Z., and L.-J. C. writing—review and editing; J. G., T.-H. C., and L.-J. C. methodology; J. G., T.-H. C., and L.-J. C. formal analysis; J. G. writing—original draft; J. Z. and H. Z. participated in study discussion.

*Conflict of interest*—The authors declare that they have no conflicts of interest with the contents of this article.

*Abbreviations*—The abbreviations used are: AAV, Adeno-associated virus vector; Abs, antibodies; aPTT, activated Partial Thromboplastin Time; BDD, B-domain deleted; BM, bone marrow; coIP, coimmunoprecipitation; ECs, endothelial cells; ER, endoplasmic reticulum; F8, factor FVIII; F8-N8, eight specific N-glycosylation sites; fF8, full-length F8; gDNA, genomic DNA; HA, hemophilia A; Hb, hemoglobin; hF8, human F8; HSCT, HSC transplantation; L, lysates; LV, lentiviral vector/lentivirus; mAb, monoclonal antibody; mHSC, murine/mouse hematopoietic stem cell; MOI, multiplicities of infection; PRT, protein replacement therapy; qPCR, quantitative PCR; S, supernatants; VCN, vector copy number; vWF, von Willebrand Factor; WB, Western blotting.

### References

1. Soucie, J. M., Evatt, B., and J Ac Kson, D. (2010) Occurrence of hemophilia in the United States. *Am. J. Hematol.* **59**, 288–294
2. Croteau, S. E., Wang, M., and Wheeler, A. P. (2021) 2021 clinical trials update: Innovations in hemophilia therapy. *Am. J. Hematol.* **96**, 128–144
3. Guo, X. L., Chung, T. H., Qin, Y., Zheng, J., Zheng, H., Sheng, L., Wynn, T., and Chang, L.-J. (2019) Hemophilia gene therapy: New development from bench to bed side. *Curr. Gene Ther.* **19**, 264–273
4. Rangarajan, S., Walsh, L., Lester, W., Perry, D., Madan, B., Laffan, M., Yu, H., Vettermann, C., Pierce, G. F., Wong, W. Y., and Pasi, K. J. (2017) AAV5-Factor VIII gene transfer in severe hemophilia A. *N. Engl. J. Med.* **377**, 2519–2530
5. Pasi, K. J., Rangarajan, S., Mitchell, N., Lester, W., Symington, E., Madan, B., Laffan, M., Russell, C. B., Li, M., Pierce, G. F., and Wong, W. Y. (2020) Multiyear follow-up of AAV5-hFVIII-SQ gene therapy for hemophilia A. *N. Engl. J. Med.* **382**, 29–40
6. Mannucci, P. M., and Tuddenham, E. G. D. (2001) The hemophilias - from royal genes to gene therapy. *N. Engl. J. Med.* **344**, 1773–1779
7. Kumar, H. P., Hague, C., Haley, T., Starr, C. M., Besman, M. J., Lundblad, R. L., and D. B. (2011) Elucidation of N-linked oligosaccharide structures of recombinant human factor VIII using fluorophore-assisted carbohydrate electrophoresis. *Biotechnol. Appl. Biochem.* **24**, 207–216

8. Miao, H. Z., Sirachainan, N., Palmer, L., Kucab, P., Cunningham, M. A., Kaufman, R. J., and Pipe, S. W. (2004) Bioengineering of coagulation factor VIII for improved secretion. *Blood* **103**, 3412–3419
9. Cerullo, V., Seiler, M. P., Mane, V., Cela, R., Clarke, C., Kaufman, R. J., Pipe, S. W., and Lee, B. (2007) Correction of murine hemophilia A and immunological differences of factor VIII variants delivered by helper-dependent adenoviral vectors. *Mol. Ther.* **15**, 2080–2087
10. Pan, J., Dinh, T. T., Rajaraman, A., Lee, M., and Butcher, E. C. (2016) Patterns of expression of factor VIII and von Willebrand factor by endothelial cell subsets *in vivo*. *Blood* **128**, 104
11. Chang, L.-J., and Gay, E. E. (2001) The molecular genetics of lentiviral vectors - current and future perspectives. *Curr. Gene Ther.* **1**, 237–251
12. Shi, Q., Kuether, E. L., Chen, Y., Schroeder, J. A., and Montgomery, R. R. (2014) Platelet gene therapy corrects the hemophilic phenotype in immunocompromised hemophilia A mice transplanted with genetically manipulated human cord blood stem cells. *Blood* **123**, 395–403
13. Toole, J. J., Pittman, D. D., Orr, E. C., Murtha, P., Wasley, L. C., and Kaufman, R. J. (1986) A large region (approximately equal to 95 kDa) of human factor VIII is dispensable for *in vitro* procoagulant activity. *Proc. Natl. Acad. Sci. U. S. A.* **83**, 5939–5942
14. Eaton, D. L., Hass, P. E., Riddle, L., Mather, J., Wiebe, M., Gregory, T., and Vehar, G. A. (1987) Characterization of recombinant human factor VIII. *J. Biol. Chem.* **262**, 3285–3290
15. Kaufman, R. J., Wasley, L. C., and Dorner, A. (1988) Synthesis, processing, and secretion of recombinant human factor VIII expressed in mammalian cells. *J. Biol. Chem.* **263**, 6352–6362
16. Titani, K., Kumar, S., Takio, K., Ericsson, L. H., Wade, R. D., Ashida, K., Walsh, K. A., Chopek, M. W., Sadler, J. E., and Fujikawa, K. (1986) Amino acid sequence of human von Willebrand factor. *Biochemistry* **25**, 3171–3184
17. Weiss, H. J., Sussman, I. I., and Hoyer, L. W. (1977) Stabilization of factor VIII in plasma by the von Willebrand Factor. *J. Clin. Invest.* **60**, 390–404
18. Samelson-Jones, B. J., and Arruda, V. R. (2018) Protein-engineered coagulation factors for hemophilia gene therapy. *Mol. Ther Methods Clin. D* **12**, 184
19. Nathwani, A. C., Reiss, U. M., Tuddenham, E. G. D., Rosales, C., Chowdhury, P., McIntosh, J., Della Peruta, M., Lheriteau, E., Patel, N., Raj, D., Riddell, A., Pie, J., Rangarajan, S., Bevan, D., Recht, M., *et al.* (2014) Long-term safety and efficacy of factor IX gene therapy in hemophilia B. *N. Engl. J. Med.* **371**, 1994–2004
20. Weber, A., Engelmaier, A., Voelkel, D., Pachlinger, R., and Rottensteiner, H. (2018) Development of methods for the selective measurement of the single amino acid exchange variant coagulation factor IX padua. *Mol. Ther Methods Clin. D* **10**, 29–37
21. Pittman, D. D., Alderman, E. M., Tomkinson, K. N., Wang, J. H., Giles, A. R., and Kaufman, R. J. (1993) Biochemical, immunological, and *in vivo* functional characterization of B-domain-deleted factor VIII. *Blood* **81**, 2925–2935
22. Dorner, A. J., Bole, D. G., and Kaufman, R. J. (1987) The relationship of N-linked glycosylation and heavy chain-binding protein association with the secretion of glycoproteins. *J. Cell Biol.* **105**, 2665–2674
23. Crawford, B., Ozelo, M. C., Ogiwara, K., Ahlin, J., Albanez, S., Hegadorn, C., Harpell, L., Hough, C., and Lillicrap, D. (2015) Transgene-host cell interactions mediate significant influences on the production, stability, and function of recombinant canine FVIII. *Mol. Ther Methods Clin. D* **2**, 15033
24. Ward, N. J., Buckley, S. M. K., Waddington, S. N., Vandendriessche, T., Chuah, M. K. L., Nathwani, A. C., McIntosh, J., Tuddenham, E. G. D., Kinnon, C., and Thrasher, A. J. (2011) Codon optimization of human factor VIII cDNAs leads to high-level expression. *Blood* **117**, 798
25. Fay, P. J. (2004) Activation of factor VIII and mechanisms of cofactor action. *Blood Rev.* **18**, 1–15
26. Gale, A. J., Cramer, T. J., Rozenshteyn, D., and Cruz, J. R. (2008) Detailed mechanisms of the inactivation of factor VIIIa by activated protein C in the presence of its cofactors, protein S and factor V. *J. Biol. Chem.* **283**, 16355–16362
27. Graw, J., Brackmann, H.-H., Oldenburg, J., Schneppenheim, R., Spannagl, M., and Schwaab, R. (2005) Haemophilia A: From mutation analysis to new therapies. *Nat. Rev. Genet.* **6**, 488–501
28. Plantier, J. L., Rolli, V., Ducasse, C., Dargaud, Y., Enjolras, N., Boukerche, H., and Negrier, C. (2010) Activated factor X cleaves factor VIII at arginine 562, limiting its cofactor efficiency. *J. Thromb. Haemost.* **8**, 286–293
29. Shahani, T., Covens, K., Lavend'homme, R., Jazouli, N., Sokal, E., Peerlinck, K., and Jacquemin, M. (2014) Human liver sinusoidal endothelial cells but not hepatocytes contain factor VIII. *J. Thromb. Haemost.* **12**, 36–42
30. Everett, L. A., Cleuren, A. C. A., Khoriaty, R. N., and Ginsburg, D. (2014) Murine coagulation factor VIII is synthesized in endothelial cells. *Blood* **123**, 3697–3705
31. Fahs, S. A., Hille, M. T., Shi, Q., Weiler, H., and Montgomery, R. R. (2014) A conditional knockout mouse model reveals endothelial cells as the principal and possibly exclusive source of plasma factor VIII. *Blood* **123**, 3706–3713
32. Merlin, S., Famà, R., Borroni, E., Zanolini, D., Brusca, G., Zucchelli, S., and Follenzi, A. (2019) FVIII expression by its native promoter sustains long-term correction avoiding immune response in hemophilic mice. *Blood Adv.* **3**, 825–838
33. Liu, L., Xia, S., and Seifert, J. (1994) Transplantation of spleen cells in patients with hemophilia A. A report of 20 cases. *Transpl. Int.* **7**, 201–206
34. Sahud, M. A. (1970) Dextropropoxyphene in bleeding states. *N. Engl. J. Med.* **283**, 48
35. Mckee, P. A., Coussons, R. T., Buckner, R. G., Williams, G. R., and Hampton, J. W. (1970) Effects of the spleen on canine factor VIII levels. *J. Lab. Clin. Med.* **75**, 391
36. Jiang, H. C., Gao, Y., Dai, W. J., Sun, B., Xu, J., Qiao, H. Q., Meng, Q. H., and Wu, C. J. (2006) Ten-year experience with living related donated splenic transplantation for the treatment of hemophilia A. *Transplant. Proc.* **38**, 1483–1490
37. Bastos, J. L., Faerstein, E., Celeste, R. K., and Barros, A. J. (2012) Explicit discrimination and health: Development and psychometric properties of an assessment instrument. *Rev. Saude Publica* **46**, 269–278
38. Kumaran, V., Bente, D., Follenzi, A., Joseph, B., Sarkar, R., and Gupta, S. (2005) Transplantation of endothelial cells corrects the phenotype in hemophilia A mice. *J. Thromb. Haemost.* **3**, 2022–2031
39. Zanolini, D., Merlin, S., Feola, M., Rinaldo, G., Amoroso, A., Gaidano, G., Zaffaroni, M., Ferrero, A., Brunelleschi, S., Valente, G., Gupta, S., Prat, M., and Follenzi, A. (2015) Extrahepatic sources of factor VIII potentially contribute to the coagulation cascade correcting the bleeding phenotype of mice with hemophilia A. *Haematologica* **100**, 881–892
40. Follenzi, A., Raut, S., Merlin, S., Sarkar, R., and Gupta, S. (2012) Role of bone marrow transplantation for correcting hemophilia A in mice. *Blood* **119**, 5532–5542
41. Lin, Y., Weisdorf, D., Solovey, A., and Heibel, R. P. (2000) Origins of circulating endothelial cells and endothelial outgrowth from blood. *J. Clin. Invest.* **105**, 71–77
42. Wang, X., Shin, S. C., Chiang, A. F., Khan, I., Pan, D., Rawlings, D. J., and Miao, C. H. (2015) Intraosseous delivery of lentiviral vectors targeting factor VIII expression in platelets corrects murine hemophilia A. *Mol. Ther.* **23**, 617–626
43. Miao, C. H. (2016) Hemophilia A gene therapy via intraosseous delivery of factor VIII-lentiviral vectors. *Thromb. J.* **14**, 41
44. Wang, X., Fu, R. Y., Li, C., Chen, C. Y., Firman, J., Konkle, B. A., Zhang, J., Li, L., Xiao, W., Poncz, M., and Miao, C. H. (2020) Enhancing therapeutic efficacy of *in vivo* platelet-targeted gene therapy in hemophilia A mice. *Blood Adv.* **4**, 5722–5734
45. Barrow, R. T., Healey, J. F., Jacquemin, M. G., Saint-Remy, J. M., and Lollar, P. (2001) Antigenicity of putative phospholipid membrane-binding residues in factor VIII. *Blood* **97**, 169–174
46. Doering, C. B., Healey, J. F., Parker, E. T., Barrow, R. T., and Lollar, P. (2002) High level expression of recombinant porcine coagulation factor VIII. *J. Biol. Chem.* **277**, 38345–38349
47. Chang, L.-J., Urlacher, V., Iwakuma, T., Cui, Y., and Zucali, J. (1999) Efficacy and safety analyses of a recombinant human immunodeficiency virus type 1 derived vector system. *Gene Ther.* **6**, 715–728
48. Iwakuma, T., Cui, Y., and Chang, L.-J. (1999) Self-inactivating lentiviral vectors with U3 and U5 modifications. *Virology* **261**, 120–132

49. Chen, X., He, J., and Chang, L.-J. (2004) Alteration of T cell immunity by lentiviral transduction of human monocyte-derived dendritic cells. *Retrovirology* **1**, 37
50. Chang, L.-J. (2010) Lentiviral vector transduction of dendritic cells for novel vaccine strategies. *Methods Mol. Biol.* **614**, 161–171
51. Nováková, I., Mensink, E., Verbeek, K., Samis, J., Giles, A., and Verbruggen, B. (2017) The type of factor VIII deficient plasma used influences the performance of the Nijmegen modification of the Bethesda assay for factor VIII inhibitors. *Thromb. Haemost.* **86**, 1435–1439
52. Liu, Y., Jennings, N. L., Dart, A. M., and Du, X. J. (2012) Standardizing a simpler, more sensitive and accurate tail bleeding assay in mice. *World J. Exp. Med.* **2**, 30–36
53. Follenzi, A., Benten, D., Novikoff, P., Faulkner, L., Raut, S., and Gupta, S. (2008) Transplanted endothelial cells repopulate the liver endothelium and correct the phenotype of hemophilia A mice. *J. Clin. Invest.* **118**, 935–945